

Constraining the symmetry energy content of nuclear matter from nuclear masses: a covariance analysis

C. Mondal, B. K. Agrawal, and J. N. De

Saha Institute of Nuclear Physics, 1/AF Bidhannagar, Kolkata 700064, India

Elements of nuclear symmetry energy evaluated from different energy density functionals parametrized by fitting selective bulk properties of few representative nuclei are seen to vary widely. Those obtained from experimental data on nuclear masses across the periodic table, however, show that they are better constrained. A possible direction in reconciling this paradox may be gleaned from comparison of results obtained from use of the binding energies in the fitting protocol within a microscopic model with two sets of nuclei, one a representative standard set and another where very highly asymmetric nuclei are additionally included. A covariance analysis reveals that the additional fitting protocol reduces the uncertainties in the nuclear symmetry energy coefficient, its slope parameter as well as the neutron-skin thickness in ^{208}Pb nucleus by $\sim 50\%$. The central values of these entities are also seen to be slightly reduced.

PACS numbers: 21.30.Fe, 21.65.Ef, 21.60.Jz

I. INTRODUCTION

Constraining quantitatively the symmetry energy C_v^0 of nuclear matter at saturation density ρ_0 and its density slope $L_0 (= 3\rho_0 \frac{\partial C_v(\rho)}{\partial \rho} |_{\rho_0})$ has been a major focus of attention in present-day nuclear physics. They are fundamental parameters in influencing the binding energies and stability of atomic nuclei and in shaping the isospin distributions there giving rise to neutron-skins (Δr_{np}) in nuclei of large neutron excess [1–3], where Δr_{np} is the difference between the rms radii for density distributions of the neutrons and protons in a nucleus. They are also of seminal importance in astronomical context. The interplay of gravitation with the pressure of neutron matter $P_n (= 3\rho_0 L_0)$ at ρ_0 is a determining factor in the radii of neutron stars [4]. The dynamical evolution of the core-collapse of a massive star and the associated explosive nucleosynthesis depend sensitively on the slope parameter L_0 [5, 6]. It also controls the nature and stability of phases within a neutron star, its critical composition, thickness and frequencies of crustal vibration [7] and determines the feasibility of direct Urca cooling processes within its interior [5, 8, 9].

The value of the symmetry energy coefficient C_v^0 has been known for some decades to be in the range of $\sim 32.0 \pm 4.0$ MeV [10–13]. In a controlled finite-range droplet model (FRDM) from a fit of the observed nuclear masses, the uncertainty in its value shrunk appreciably, it was found to be $C_v^0 = 32.5 \pm 0.5$ MeV [3]. Studying meticulously the double differences of symmetry energies estimated from experimental nuclear masses, Jiang *et al* [14] find its value to be 32.10 ± 0.31 MeV. Their procedure takes advantage of the fact that other effects like pairing and shell corrections in symmetry energy are well cancelled out from double differences of neighboring nuclei.

Initial explorations on the symmetry slope L_0 , however, show wide variations. The suggested lower limit is ~ 20 MeV, on the high side, it is ~ 120 MeV [15]. Astro-

physical observations of neutron star radii and masses provide [16] a value of L_0 between 43 and 52 MeV, though. On the other hand, correlation systematics of Δr_{np} with nuclear isospin [15], isoscaling [17], nucleon emission ratios [18], isospin diffusion [19] in heavy-ion collision, analysis of giant dipole resonance of ^{208}Pb [20, 21], giant quadrupole resonance in ^{208}Pb [22], pigmy dipole resonance in ^{68}Ni and ^{132}Sn [23] or of nuclear ground state properties using the standard Skyrme Hartree-Fock approach [24], all yield values of L_0 that differ substantially from one another [25]. Efforts have also been made to constrain the value of L_0 by fitting the binding energies of large number of deformed nuclei within the density dependent point coupling model [26, 27] and by considering the pseudo data on the equation of state for the asymmetric nuclear matter or pure neutron matter in the fitting protocol of the Skyrme models [28, 29] as well as the density dependent meson exchange models [30]. These studies indicate that L_0 is in the range of 40 - 70 MeV.

Analysis of data on the nuclear masses in macroscopic models seems to contain the fluctuations in the value of L_0 somewhat better. In a macroscopic nuclear model such as liquid drop, surface tension tends to favor a nearly uniform drop of neutrons and protons. For a nucleus, say, with large neutron excess it is energetically advantageous to distribute some neutrons out at the surface of reduced density (where the symmetry energy is lower) giving rise to a neutron skin. Imprints of symmetry energy coefficient C_v^0 and its density slope L_0 are thus encoded in the precisely known nuclear masses. Fitting the few thousand observed nuclear masses within the FRDM [3], the value of L_0 was found to be 70 ± 15 MeV. The surface symmetry coefficient C_s , along with C_v^0 might also be used to estimate the value of L_0 [5, 15]. Consistent with the values of C_v^0 and C_s (as determined from double differences of symmetry energies estimated from experimental nuclear masses [14] to be 58.91 ± 1.08 MeV), a recent effort aided by microscopic calculations on the Δr_{np} of

TABLE I: The best fit values for the parameters of model-I and model-II. m_σ is the mass of σ meson given in units of MeV. The masses of ω and ρ mesons are kept fixed to $m_\omega = 782.5$ MeV and $m_\rho = 763$ MeV and nucleon mass is taken to be $M = 939$ MeV. Uncorrelated errors on the fitted parameters (upper line) and total correlated errors on them (lower line) are given inside the parenthesis for both the models.

Name	g_σ	g_ω	g_ρ	κ_3	κ_4	$\eta_{2\rho}$	ζ_0	m_σ
model-I	-10.62457 (0.00013) (0.246)	13.8585 (0.0002) (0.662)	12.077 (0.045) (2.60)	1.46285 (0.00024) (0.275)	-0.9673 (0.0024) (3.66)	28.33 (0.47) (29.9)	5.2056 (0.0027) (3.21)	496.0067 (0.0062) (12.2)
model-II	-10.62123 (0.00011) (0.149)	13.85989 (0.00017) (0.262)	12.436 (0.046) (1.54)	1.46223 (0.00021) (0.290)	-0.8566 (0.0022) (1.53)	32.50 (0.49) (18.1)	5.3220 (0.0027) (0.099)	495.8146 (0.0054) (8.23)

heavy nuclei [31–33] gives $L_0 = 59 \pm 13$ MeV. This is not far from the one ($L_0 = 65.5 \pm 13.5$ MeV) obtained from the nuclear equation of state (EoS) constructed [34] from some well-accepted empirical macroscopic nuclear constraints. Exploiting nuclear masses thus seems more or less to constrain better the symmetry elements C_v^0 and L_0 of nuclear matter.

in the exploration of nuclear masses in microscopic models. For example in the study [37] of the binding energy difference ΔB of ^{132}Sn and ^{100}Sn (which is sensitive to the symmetry energy content) vis a vis the neutron skin Δr_{np} of ^{132}Sn for different sets of Skyrme EDFs, no noticeable correlation between ΔB and Δr_{np} was found. The different EDFs reproduce the binding energy difference fairly well, but the value of Δr_{np} differ in a wide range.

This quizzical finding leaves open the understanding on the incompatibility of the tighter constraints on the symmetry energy coefficients of nuclear matter extracted from experimental nuclear masses with the larger uncertainties on the values of C_v^0 and L_0 as obtained from parametrizations of the microscopic mean field models. The purpose of this communication is to give a general direction in shading light on this seeming paradox. In an exploratory calculation, we show that the apparent irreconciliation can be eased if some highly asymmetric even-even spherical nuclei are additionally included in the fitting protocol of the optimization of the EDFs in microscopic mean field models. The relativistic mean-field model (RMF) is chosen as the vehicle for the realization of our goal.

To keep the matter simple yet pointed, we exploit the binding energy difference between four pairs of nuclei in different RMF models showing increasing asymmetry effects: ($^{68}\text{Ni} - ^{56}\text{Ni}$), ($^{132}\text{Sn} - ^{100}\text{Sn}$), ($^{24}\text{O} - ^{16}\text{O}$) and ($^{30}\text{Ne} - ^{18}\text{Ne}$). The neutron rich ^{68}Ni and ^{132}Sn nuclei have asymmetries $\delta = 0.176$ and 0.242 respectively (δ is the isospin asymmetry parameter $(N - Z)/A$); ^{24}O and ^{30}Ne have $\delta = 0.3$. The Ni and Sn isotopes are doubly closed shell nuclei. So also the O-nuclei, ^{24}O is recently seen to be an unexpectedly stable doubly magic nucleus [38, 39]. The Ne-nuclei have their neutron shells closed but have valence protons. The binding energy difference between the two Ne-nuclei is expected to cancel the pairing and the possible core-polarization effects arising from the two valence protons partially. In Fig.1 the binding energy difference between the four pairs of nuclei are plotted against Δr_{np} of ^{208}Pb , the Δr_{np} and the binding energies being calculated for seven models of BSR family [40, 41], NL3 [42], FSU [8] and for seven models

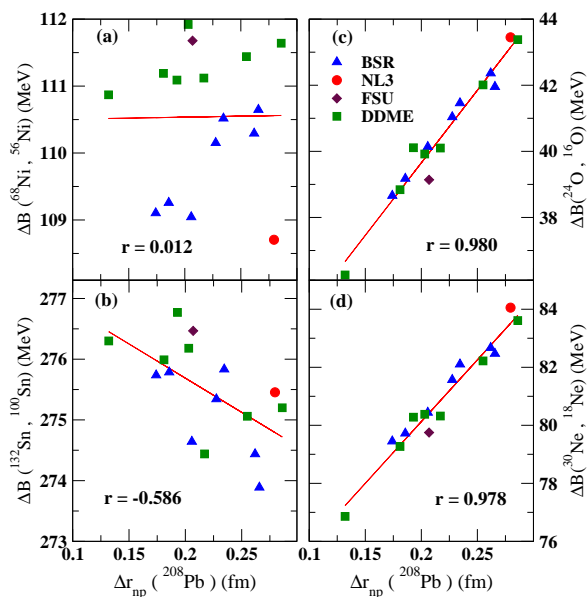


FIG. 1: (Color online) The binding energy difference $\Delta B(X, Y) = B(X) - B(Y)$ for four different pairs of isotopes are plotted against neutron-skin thickness Δr_{np} in the ^{208}Pb nucleus for 16 different RMF models (See text for details). The values of Pearson's correlation coefficients r are also displayed.

Energy density functionals (EDF) in microscopic mean field models, parametrized to reproduce the binding energies of nuclei alongwith some other specific nuclear observables do not, however, display such constraints on the symmetry elements of nuclear matter. The EoS constructed out of the different EDFs show wide variations in the value of C_v^0 and L_0 [35, 36]. Questions then arise how the information content of symmetry energy gets blurred

of Density Dependent Meson Exchange (DDME) family [43]. The correlation coefficient for the Ni-pair is seen to be only 0.012, for the Sn-pair, it has increased to 0.586. For the O and Ne pairs, they are quite high, 0.980 and 0.978, respectively. One can not but fail to notice the increasingly high correlation with increasing asymmetry, particularly for the latter two cases.

The occurrence of strong correlation for the case of O and Ne pairs probably suggest that selective combination of suitable binding energies of nuclei of low and high isospin may be ideally suited to better constrain the isovector part of the nuclear interaction. A covariance analysis uncovers correlations among the physical observables; revelation of this interdependence may be of great importance in assigning values to the physical observables of interest with statistical uncertainties. We aim to do that presently, the observables we explore are those that carry the imprint of isovector content of nuclear interaction i.e. the symmetry energy C_v^0 and the symmetry energy slope L_0 along with the Δr_{np} of ^{208}Pb .

II. EFFECTIVE LAGRANGIAN

The effective Lagrangian density for the RMF model employed in the present work is similar to that of the FSU one [8, 44–46]. The interaction part of the Lagrangian can be written as,

$$\begin{aligned} \mathcal{L}_{int} = & \bar{\psi} \left[g_\sigma \sigma - \gamma^\mu \left(g_\omega \omega_\mu + \frac{1}{2} g_\rho \tau \cdot \rho_\mu + \frac{e}{2} (1 + \tau_3) A_\mu \right) \right] \psi \\ & - \frac{\kappa_3}{6M} g_\sigma m_\sigma^2 \sigma^3 - \frac{\kappa_4}{24M^2} g_\sigma^2 m_\sigma^2 \sigma^4 + \frac{1}{24} \zeta_0 g_\omega^2 (\omega_\mu \omega^\mu)^2 \\ & + \frac{\eta_{2\rho}}{4M^2} g_\omega^2 m_\rho^2 \omega_\mu \omega^\mu \rho_\nu \rho^\nu. \end{aligned} \quad (1)$$

It contains the usual Yukawa coupling between the nucleonic field (ψ) and different meson fields, namely, isoscalar-scalar σ (coupling constant g_σ), isoscalar-vector ω (g_ω), isovector-vector ρ (g_ρ) and photon A^μ . The parameters κ_3 , κ_4 and ζ_0 determine the strength of self-couplings of σ and ω mesons. The self-couplings enable one to produce softening in the EoS of symmetric nuclear matter if needed. The ω - ρ cross-coupling with coupling-constant $\eta_{2\rho}$ controls the density dependence of symmetry energy.

III. FIT DATA AND MODEL PARAMETERS

The values of the parameters entering the EDF of the RMF model are obtained from an optimal χ^2 fit of the experimental observables with the theoretically calculated values. The optimal values of the parameters of the EDF give the minimum $\chi_0^2(\mathbf{p})$ of the objective function $\chi^2(\mathbf{p})$ (\mathbf{p} referring to the parameter space), defined as,

$$\chi^2(\mathbf{p}) = \frac{1}{N_d - N_p} \sum_{i=1}^{N_d} \left(\frac{\mathcal{O}_i^{exp} - \mathcal{O}_i^{th}(\mathbf{p})}{\Delta \mathcal{O}_i} \right)^2, \quad (2)$$

where, N_d and N_p are the number of experimental data points and the number of fitted parameters, respectively. $\Delta \mathcal{O}_i$ is the adopted error and \mathcal{O}_i^{exp} and $\mathcal{O}_i^{th}(\mathbf{p})$ are the experimental and the corresponding theoretical values for a given observable. The values of $\Delta \mathcal{O}_i$ are chosen in such a way that $\chi_0^2(\mathbf{p})$ is unity. The experimental observables, in our case, include only the values of the binding energies and charge radii of a selected set of nuclei. There may be values of parameters that are also likely, they can give a reasonable fit to the data, the reasonableness of the domain of parameter space being defined as $\chi^2(\mathbf{p}) \leq \chi_0^2(\mathbf{p}) + 1$ [47–49]. A reasonable domain of parameters yields a reasonable set of results for each set of predicted observables.

To explore the results of Fig.1 more critically, two models (model-I and model-II) corresponding to different sets of fit-data are constructed. In model-I the binding energies and charge radii of some standard set of nuclei (^{16}O , ^{40}Ca , ^{48}Ca , ^{56}Ni , ^{68}Ni , ^{90}Zr , ^{100}Sn , ^{116}Sn , ^{132}Sn , ^{144}Sm and ^{208}Pb) spanning the entire periodic table are taken as fit-data. In model-II, we have the same set of experimental observables, but with the addition of the binding energy difference ΔB of (^{24}O , ^{16}O) and of (^{30}Ne , ^{18}Ne). The parameters of model-I and model-II are obtained by optimizing [50] the objective function $\chi^2(\mathbf{p})$ as given by Eq. (2).

Once the optimized parameter set is obtained the correlation coefficient between two quantities \mathcal{A} and \mathcal{B} , which may be a parameter as well as an observable, can be evaluated within the covariance analysis as,

$$c_{AB} = \frac{\overline{\Delta \mathcal{A} \Delta \mathcal{B}}}{\sqrt{\overline{\Delta \mathcal{A}^2} \overline{\Delta \mathcal{B}^2}}}, \quad (3)$$

where, covariance between \mathcal{A} and \mathcal{B} is expressed as,

$$\overline{\Delta \mathcal{A} \Delta \mathcal{B}} = \sum_{\alpha\beta} \left(\frac{\partial \mathcal{A}}{\partial p_\alpha} \right)_{\mathbf{p}_0} C_{\alpha\beta}^{-1} \left(\frac{\partial \mathcal{B}}{\partial p_\beta} \right)_{\mathbf{p}_0}. \quad (4)$$

Here, $C_{\alpha\beta}^{-1}$ is an element of inverted curvature matrix given by,

$$C_{\alpha\beta} = \frac{1}{2} \left(\frac{\partial^2 \chi^2(\mathbf{p})}{\partial p_\alpha \partial p_\beta} \right)_{\mathbf{p}_0}, \quad (5)$$

where, \mathbf{p}_0 represents the optimized set of parameters. The square of the error, $\overline{\Delta \mathcal{A}^2}$ in \mathcal{A} can be computed using Eq. (4) by substituting $\mathcal{B} = \mathcal{A}$. Curvature matrix can also facilitate to locate the reasonable domain of parameters [4, 49, 51]. The parameters for model-I and II corresponding to minimum value of the objective function $\chi^2(\mathbf{p})$ ($=\chi_0^2(\mathbf{p})$) along with their uncorrelated and correlated statistical errors are listed in Table I. The correlated and uncorrelated errors are computed with and without contributions from the non-diagonal elements of the matrix \mathcal{C} as given by Eq. 5, respectively. The correlated errors on the parameters for the case of model-II are smaller than those obtained for the model-I indicating that the inclusion of the fit data on the binding

TABLE II: Observables \mathcal{O} of different nuclei, adopted errors on them $\Delta\mathcal{O}$, their experimental values and the ones obtained for model-I and II. B and r_{ch} refers to binding energy and charge radius of a nucleus respectively, and ΔB is binding energy difference of two isotopes of a nucleus as indicated. B and ΔB are in units of MeV and r_{ch} in fm.

Nucleus	\mathcal{O}	$\Delta\mathcal{O}$	Expt.	model-I	model-II
^{16}O	B	4.0	127.62	127.781 ± 0.990	127.783 ± 0.576
	r_{ch}	0.04	2.701	2.700 ± 0.017	2.699 ± 0.013
$^{16}\text{O}, ^{24}\text{O}$	ΔB	2.0	41.34	-	40.995 ± 1.046
$^{18}\text{Ne}, ^{30}\text{Ne}$	ΔB	2.0	79.147	-	79.149 ± 1.296
	B	3.0	342.051	342.929 ± 1.064	342.927 ± 0.927
^{40}Ca	r_{ch}	0.02	3.478	3.457 ± 0.013	3.455 ± 0.010
	B	1.0	415.99	414.883 ± 0.720	414.751 ± 0.541
^{48}Ca	r_{ch}	0.04	3.479	3.439 ± 0.007	3.439 ± 0.006
	B	5.0	483.99	483.752 ± 2.495	483.619 ± 1.646
^{56}Ni	r_{ch}	0.18	3.750	3.695 ± 0.025	3.693 ± 0.020
	B	1.0	590.43	592.294 ± 0.784	592.162 ± 0.736
^{68}Ni	B	1.0	590.43	592.294 ± 0.784	592.162 ± 0.736
	r_{ch}	0.02	4.269	4.267 ± 0.009	4.267 ± 0.034
^{90}Zr	B	1.0	783.893	782.855 ± 4.833	782.776 ± 1.621
	r_{ch}	0.02	4.269	4.267 ± 0.009	4.267 ± 0.034
^{100}Sn	B	2.0	825.8	827.987 ± 1.753	827.757 ± 1.534
	r_{ch}	0.18	4.626	4.623 ± 0.009	4.623 ± 0.008
^{116}Sn	B	2.0	988.32	987.169 ± 0.946	987.072 ± 0.760
	r_{ch}	0.02	4.71	4.711 ± 0.011	4.712 ± 0.010
^{132}Sn	B	1.0	1102.9	1102.851 ± 1.146	1102.631 ± 0.856
	r_{ch}	0.02	4.71	4.711 ± 0.011	4.712 ± 0.010
^{144}Sm	B	2.0	1195.74	1195.834 ± 1.240	1195.736 ± 1.287
	r_{ch}	0.02	4.96	4.956 ± 0.009	4.956 ± 0.009
^{208}Pb	B	1.0	1636.446	1636.457 ± 4.301	1636.383 ± 0.917
	r_{ch}	0.02	5.504	5.530 ± 0.012	5.531 ± 0.010

energy differences constrain the model parameters better. In particular, the errors on the parameters g_ρ and $\eta_{2\rho}$, which govern the isovector part of the effective Lagrangian, are smaller for the model-II. The large error on the parameters κ_3 and κ_4 for both the models may be due to the fact that the fit data does not include any observable which could constrain the value of the nuclear matter incompressibility coefficient [46]. In Table II different observables \mathcal{O}_i , adopted errors on them $\Delta\mathcal{O}_i$, their experimental values along with the results obtained for model-I and model-II using the corresponding best fit parameters are listed. The values of \mathcal{O}_i and $\Delta\mathcal{O}_i$, except for the ΔB of ($^{24}\text{O}, ^{16}\text{O}$) and ($^{30}\text{Ne}, ^{18}\text{Ne}$) and r_{ch} of ^{132}Sn , are exactly same as used in Ref. [52]. The experimental data for ΔB of ($^{24}\text{O}, ^{16}\text{O}$) and ($^{30}\text{Ne}, ^{18}\text{Ne}$) are taken from [53] and that for the r_{ch} of ^{132}Sn from [54].

IV. RESULTS AND DISCUSSIONS

We now compare the results obtained for the model-I and model-II to see upto what extent the inclusion of the experimental data on the binding energy differences between the pair of O and Ne nuclei can constrain the iso-vector part of the effective Lagrangian. In Fig. 2(a) the reasonable domain for the parameters g_ρ and $\eta_{2\rho}$ is

TABLE III: The values for the binding energy per nucleon E/A , incompressibility coefficient K , Dirac effective mass of nucleon m^*/m , symmetry energy coefficient C_v^0 and density slope parameter of symmetry energy L_0 for the nuclear matter evaluated at saturation density ρ_0 along with the correlated errors on them obtained within the covariance analysis for the models I and II. The results for neutron-skin thickness Δr_{np} in ^{48}Ca , ^{132}Sn and ^{208}Pb are also presented.

Observable	model-I	model-II
E/A (MeV)	-16.036 ± 0.070	-16.036 ± 0.051
K (MeV)	210.12 ± 27.87	209.64 ± 28.52
ρ_0 (fm^{-3})	0.150 ± 0.003	0.150 ± 0.003
m^*/m	0.585 ± 0.012	0.585 ± 0.010
C_v^0 (MeV)	32.03 ± 3.08	31.69 ± 1.51
L_0 (MeV)	57.62 ± 17.08	55.63 ± 7.00
Δr_{np} (^{48}Ca) (fm)	0.191 ± 0.036	0.187 ± 0.016
Δr_{np} (^{132}Sn) (fm)	0.266 ± 0.070	0.257 ± 0.031
Δr_{np} (^{208}Pb) (fm)	0.201 ± 0.065	0.193 ± 0.030

displayed. For this reasonable domain of the parameters the values of the symmetry energy slope parameter L_0 and the Δr_{np} in the ^{208}Pb nucleus are displayed in Fig. 2(b). The inclined and elongated shapes of the ellip-

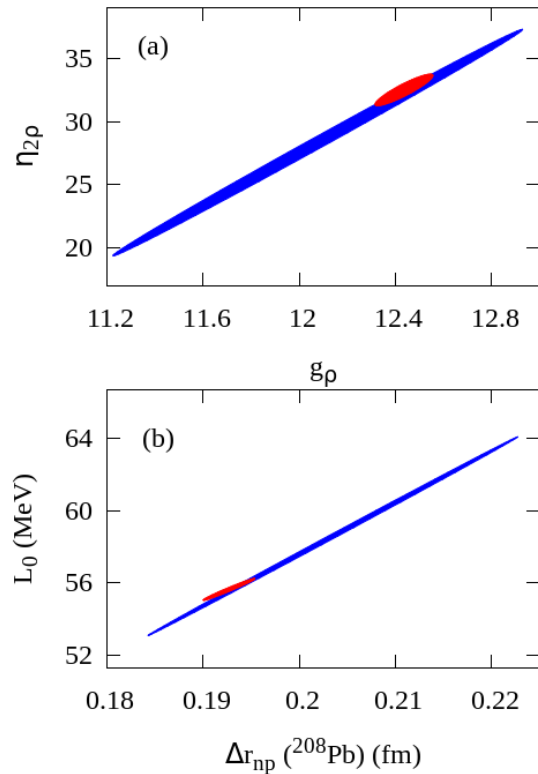


FIG. 2: (Color online) The covariance ellipsoids for the parameters $g_\rho - \eta_{2\rho}$ (upper panel) and the corresponding $L_0 - \Delta r_{np}$ (lower panel) for the model I (color blue) and model II (color red). The area inside the ellipsoids indicate the reasonable domain of the parameters.

soids indicate that the correlations amongst $g_\rho - \eta_{2\rho}$ and $L_0 - \Delta r_{np}$ are strong. In fact, the values of the correlation coefficients (Eq. (3)) for these pairs of quantities for both the models turn out to be ~ 0.95 . It is evident that the ellipsoids depicting the results for the model-II (color red) are narrower in comparison to those for the model-I (color blue). This is suggestive of the fact that the inclusion of the binding energies for the ^{24}O and ^{30}Ne put tighter constraints on the isovector part of the effective Lagrangian density.

Nuclear matter properties for model-I and model-II are compared in Table III. Errors on the entities describing the isoscalar behavior of nuclear matter (E/A , K , ρ_0 and m^*/m) are pretty much the same for both the models concerned. For model-II, however, a significant improvement (by a factor ~ 2) on the spread of parameters like C_v^0 and L_0 , which describe the symmetry behavior of

nuclear matter, is achieved over model-I. Strikingly, the errors on C_v^0 and L_0 for the model-II agree very well with the ones obtained for the SAMi Skyrme force [29] which includes the variational EoS for the pure neutron matter as pseudo data in the fitting protocol. We also provide the values of Δr_{np} for ^{48}Ca , ^{132}Sn and ^{208}Pb nuclei in Table III. The reduction in the errors on Δr_{np} for the model-II in comparison to those for the model-I are in harmony with the results depicted in Fig. 2.

To this end, it may be mentioned that the correlations of neutron-skin thickness in ^{208}Pb nucleus with L_0 has been studied within the covariance approach for different nuclear energy density functionals [55]. These correlations exhibit some degree of model dependence. In view of this, the present investigation should be extended to other energy density functionals. The value of L_0 might also be constrained by including in the fitting protocol the experimental data for the iso-vector giant dipole polarizability for the ^{208}Pb nucleus [48]. However, it must be reminded that the L_0 is well correlated with the product of dipole polarizability and the symmetry energy coefficient at the saturation density C_v^0 rather than the dipole polarizability alone [21].

V. SUMMARY AND CONCLUSION

To summarize, we have tried to give a critical look on the question why the information content on the elements of symmetry energy do not get transported properly in the EDFs when they are parametrized to reproduce the binding energies of representative nuclei in a mean-field model. The asymmetry parameters are then less constrained. Working in the confines of RMF model, we find that better constraint can be achieved in the isovector part of the effective Lagrangian density and hence in the said symmetry elements if one includes, in the fitting protocol of the microscopic model binding energies of some highly asymmetric nuclei. In this preliminary investigation, comparison of results with two sets of nuclei, one a standard set and another with two additional nuclei of very high asymmetry ($\delta = 0.3$) shows a pointer in this direction. The covariance analysis yields the reduction in the uncertainties on the values of symmetry energy and its slope parameter by $\sim 50\%$ in comparison to those obtained without the inclusion of the additional nuclei in the fit data. Similar effects are also observed on the values of Δr_{np} in ^{48}Ca , ^{132}Sn and ^{208}Pb nuclei. A more detailed analysis along this direction is underway.

[1] W. D. Myers and W. J. Swiatecki, Ann. Phys. (N. Y.) **55**, 395 (1969).

[2] W. D. Myers and W. J. Swiatecki, Nucl. Phys. **A336**, 267 (1980).

[3] P. Möller, W. D. Myers, H. Sagawa, and S. Yoshida, Phys. Rev. Lett **108**, 052501 (2012).

[4] W.-C. Chen and J. Piekarewicz, arXiv:1408.4159v1 (2014).

- [5] A. W. Steiner, M. Prakash, J. M. Lattimer, and P. J. Ellis, *Phys. Rep.* **411**, 325 (2005).
- [6] H.-T. Janka, K. Langanke, A. Marek, G. Martínez-Pinedo, and B. Müller, *Phys. Rep.* **442**, 38 (2007).
- [7] A. W. Steiner, *Phys. Rev. C* **77**, 035805 (2008).
- [8] B. G. Todd-Rutel and J. Piekarewicz, *Phys. Rev. Lett.* **95**, 122501 (2005).
- [9] J. M. Lattimer, C. J. Pethick, M. Prakash, and P. Haensel, *Phys. Rev. Lett.* **66**, 2701 (1991).
- [10] W. D. Myers and W. J. Swiatecki, *Nucl. Phys.* **A81**, 1 (1966).
- [11] P. Möller, J. Nix, W. Myers, and W. Swiatecki, *Atomic Data and Nuclear Data Tables* **59**, 185 (1995).
- [12] K. Pomorski and J. Dudek, *Phys. Rev. C* **67**, 044316 (2003).
- [13] C. Xu, B.-A. Li, and L.-W. Chen, *Phys. Rev. C* **82**, 054607 (2010).
- [14] H. Jiang, G. J. Fu, Y. M. Zhao, and A. Arima, *Phys. Rev. C* **85**, 024301 (2012).
- [15] M. Centelles, X. Roca-Maza, X. Viñas, and M. Warda, *Phys. Rev. Lett.* **102**, 122502 (2009).
- [16] A. W. Steiner and S. Gandolfi, *Phys. Rev. Lett.* **108**, 081102 (2012).
- [17] D. V. Shetty, S. J. Yennello, and G. A. Souliotis, *Phys. Rev. C* **75**, 034602 (2007).
- [18] M. A. Famiano and *et. al.*, *Phys. Rev. Lett.* **97**, 052701 (2006).
- [19] B.-A. Li, L.-W. Chen, and C. M. Ko, *Phys. Rep.* **464**, 113 (2008).
- [20] L. Trippa, G. Colò, and E. Vigezzi, *Phys. Rev. C* **77**, 061304(R) (2008).
- [21] X. Roca-Maza, M. Brenna, G. Colò, M. Centelles, X. Viñas, B. K. Agrawal, N. Paar, D. Vretenar, and J. Piekarewicz, *Phys. Rev. C* **88**, 024316 (2013).
- [22] X. Roca-Maza, M. Brenna, B. K. Agrawal, P. F. Bortignon, G. Colò, L.-G. Cao, N. Paar, and D. Vretenar, *Phys. Rev. C* **87**, 034301 (2013).
- [23] A. Carbone, G. Colò, A. Bracco, L.-G. Cao, P. F. Bortignon, F. Camera, and O. Wieland, *Phys. Rev. C* **81**, 041301(R) (2010).
- [24] L.-W. Chen, *Phys. Rev. C* **83**, 044308 (2011).
- [25] M. B. Tsang, J. R. Stone, F. Camera, P. Danielewicz, S. Gandolfi, K. Hebeler, C. J. Horowitz, J. Lee, W. G. Lynch, Z. Kohley, et al., *Phys. Rev. C* **86**, 015803 (2012).
- [26] T. Nikšić, D. Vretenar, and P. Ring, *Phys. Rev. C* **78**, 034318 (2008).
- [27] P. W. Zhao, Z. P. Li, J. M. Yao, and J. Meng, *Phys. Rev. C* **82**, 054319 (2010).
- [28] E. Chabanat, P. Bonche, P. Haensel, J. Meyer, and R. Schaeffer, *Nuclear Physics A* **635**, 231 (1998).
- [29] X. Roca-Maza, G. Colò, and H. Sagawa, *Phys. Rev. C* **86**, 031306 (2012).
- [30] X. Roca-Maza, X. Viñas, M. Centelles, P. Ring, and P. Schuck, *Phys. Rev. C* **84**, 054309 (2011).
- [31] B. K. Agrawal, J. N. De, and S. K. Samaddar, *Phys. Rev. Lett.* **109**, 262501 (2012).
- [32] B. K. Agrawal, J. N. De, S. K. Samaddar, G. Colò, and A. Sulaksono, *Phys. Rev. C* **87**, 051306(R) (2013).
- [33] J. Liu, Z. Ren, C. Xu, and R. Xu, *Phys. Rev. C* **88**, 024324 (2013).
- [34] N. Alam, B. K. Agrawal, J. N. De, S. K. Samaddar, and G. Colò, *Phys. Rev. C* **90**, 054317 (2014).
- [35] M. Dutra, O. Lourenco, J. S. Sá Martins, A. Delfino, J. R. Stone, and P. D. Stevenson, *Phys. Rev. C* **85**, 035201 (2012).
- [36] M. Dutra, O. Lourenço, S. S. Avancini, B. V. Carlson, A. Delfino, D. P. Menezes, C. Providência, S. Typel, and J. R. Stone, *Phys. Rev. C* **90**, 055203 (2014).
- [37] B. A. Brown, *Phys. Rev. Lett.* **85**, 5296 (2000).
- [38] R. Kanungo and *et al.*, *Phys. Rev. Lett.* **102**, 152501 (2009).
- [39] R. V. F. Janssens, *Nature* **459**, 1069 (2009).
- [40] S. K. Dhiman, R. Kumar, and B. K. Agrawal, *Phys. Rev. C* **76**, 045801 (2007).
- [41] B. K. Agrawal, *Phys. Rev. C* **81**, 034323 (2010).
- [42] G. A. Lalazissis, J. König, and P. Ring, *Phys. Rev. C* **55**, 540 (1997).
- [43] D. Vretenar, T. Nikšić, and P. Ring, *Phys. Rev. C* **68**, 024310 (2003).
- [44] R. Furnstahl, B. D. Serot, and H.-B. Tang, *Nucl. Phys.* **A615**, 441 (1997).
- [45] J. Boguta and A. R. Bodmer, *Nucl. Phys.* **A292**, 413 (1977).
- [46] J. Boguta and H. Stoecker, *Phys. Lett.* **B120**, 289 (1983).
- [47] S. Brandt, *Statistical and Computational Methods in Data Analysis* (Springer, New York, 3rd English edition, 1997).
- [48] P.-G. Reinhard and W. Nazarewicz, *Phys. Rev. C* **81**, 051303(R) (2010).
- [49] J. Dobaczewski, W. Nazarewicz, and P.-G. Reinhard, *J. Phys. G* **41**, 074001 (2014).
- [50] P. R. Bevington, *Data Reduction and Error Analysis for the Physical Sciences* (McGraw-Hill, New York, 1969).
- [51] J. Erler and P.-G. Reinhard, arXiv:1408.0208v1 (2014).
- [52] P. Klüpfel, P.-G. Reinhard, T. J. Bürvenich, and J. A. Maruhn, *Phys. Rev. C* **79**, 034310 (2009).
- [53] G. Audi, F. G. Kondev, M. Wang, B. Pfeiffer, X. Sun, J. Blachot, and M. MacCormick, *Chin. Phys. C* **36**, 12 (2012).
- [54] I. Angeli and K. Marinova, *Atomic Data and Nuclear Data Tables* **99**, 69 (2013).
- [55] P.-G. Reinhard, J. Piekarewicz, W. Nazarewicz, B. K. Agrawal, N. Paar, and X. Roca-Maza, *Phys. Rev. C* **88**, 034325 (2013).